New Class of Time Domain Algorithms of RMS Value Measurement of Non-Coherently Sampled Signals

Martin Novotny[1], Milos Sedlacek[1]

[1] *Czech Technical University in Prague, Faculty of Electrical Engineering, Dept. of Measurement*
Technicka 2, CZ-16627 Czech Republic
phone:+420 2 2435 2177, fax: +420 2 3333 9929, e-mail: {sedlaceM, novotnm5}@fel.cvut.cz)

Abstract- This paper introduces a new and effective method of RMS value estimation in time domain. The new approach is based on signal windowing without subsequent processing in frequency domain. Examples of newly obtained analytical formulae, comparison to the classical method and extension to multi-frequency signals are presented. Both numerical simulation and measurements are used to verify the derived formulae. The first findings based on this new method were presented in [1].

I. Introduction

The RMS value can be found by processing the samples of signal either in time domain or in the frequency domain. Time domain algorithms are frequently based on period estimation, accuracy of which determines the RMS uncertainty. If the signal period is not found (or is found with low accuracy) bias of RMS occurs. The case of RMS estimation without necessity of finding signal period (or for non-integer number of periods sampled) will be analysed here.

II. Finding RMS value in time domain by the classical algorithm

RMS estimation for analogue or digitised signals is based on the relation

$$X'_{RMS} = \sqrt{\frac{1}{T_M}\int_0^{T_M} x^2(t)dt} \cong \sqrt{\frac{1}{N}\sum_{n=0}^{N-1} x^2(n)} \tag{1}$$

where T_M is time of measurement (in classical approach integer multiple of signal period) and $x(t)$ is input signal. N is number of acquired samples with $T_M = N \cdot T_S$, T_S is sampling period and X'_{RMS} is estimate of real RMS value X_{RMS}.

The measurement time can be expressed as $T_M = (M+\lambda)\cdot T_{sig}$, where M is number of integer periods sampled, T_{sig} is signal period and λ is decimal part of the last period sampled ($0 \leq \lambda < 1$). There is $X'_{RMS} = X_{RMS}$ for $\lambda = 0$ (coherent sampling), and $X'_{RMS} \neq X_{RMS}$ for $\lambda \neq 0$. The difference between X'_{RMS} and X_{RMS} is the bias of RMS measurement in time domain caused by non-coherent sampling. The relative bias of RMS estimation for sinusoidal signal can be expressed

$$\delta_{RMS} = \frac{X'_{RMS} - X_{RMS}}{X_{RMS}} = \left(\sqrt{1 - \frac{\sin(4\pi(M+\lambda)+2\varphi) - \sin(2\varphi)}{4\pi(M+\lambda)}} - 1 \right) \cdot 100\% \tag{2}$$

where φ is signal phase related to starting point of sampling.

The bias of RMS value for sinusoidal signal with $\varphi = 0°$ and 45° is shown in Fig. 1a and for sinusoidal signal with $\varphi = 90°$ and 135° is shown in Fig. 2a.

III. Finding RMS value in time domain by the new algorithm

Bias of RMS value shown in Fig.1 is caused by decimal part of signal period λT_{sig} at the end of T_M. If the signal is multiplied by a tapering window of the identical length (as is often done before processing signal in frequency domain), the weight of the part λT_{sig} will be substantially reduced.

The most popular windows are the well-known cosine windows defined as

$$w_P(n) = \sum_{i=0}^{P} a_i \cos\left(\frac{2\pi i r}{N}\right), \quad n = 0,1,2 \ldots N-1 \tag{3}$$

where N is window length, a_i are window coefficients and P is window order. The higher the window order, the lower window spectrum side lobes and the broader window spectrum main lobe.The RMS

value of the windowed and coherently sampled signal (if more than $2P + 1$ signal periods are sampled, P being the window order) is

$$X_{RMS}(w(n)\cdot x(n)) = \sqrt{\frac{1}{N}\sum_{n=0}^{N-1}\left(w(n)\cdot x(n)\right)^2} = \sqrt{nnpg}\cdot X_{RMS}(x(n)) \tag{4}$$

Here *nnpg* is normalized noise power gain [2]

$$nnpg = \frac{1}{N}\sum_{n=0}^{N-1}\left(w(n)\right)^2 \tag{5}$$

RMS bias by non-coherent sampling is substantially reduced as compared to (1) because of windowing. Bias of RMS value estimation for the cosine window can be expressed as

$$\delta_{(w)RMS} = \left(\sqrt{\left(1 - \frac{\sin(4\pi\lambda + 2\varphi) - \sin(2\varphi)}{nnpg}\right)\times C} - 1\right)\cdot 100\ \% \tag{6}$$

$$C = \frac{nnpg}{4\pi(M+\lambda)} + \sum_{i=1}^{P} a_0 a_i\left(\frac{1}{2\pi(2(M+\lambda)+i)} + \frac{1}{2\pi(2(M+\lambda)-i)}\right) + \sum_{i=1}^{P} a_i^2\left(\frac{1}{4\pi(M+\lambda+i)} + \frac{1}{4\pi(M+\lambda-i)}\right) + \\ + \sum_{i=1}^{P-1}\sum_{j=i+1}^{P}\frac{a_i a_j}{2}\left(\frac{1}{2\pi(2(M+\lambda)+(i+j))} + \frac{1}{2\pi(2(M+\lambda)-(i+j))} + \frac{1}{2\pi(2(M+\lambda)+(i-j))} + \frac{1}{2\pi(2(M+\lambda)-(i-j))}\right) \tag{7}$$

where a_i are window coefficients. The dependency of RMS bias on measurement time for sinusoidal signal with the same properties as in Fig.1a and Fig. 2a is shown in Fig.1b and Fig. 2b. Curves in Fig.1 and 2 are overlapping results of theoretical analysis and numerical simulation.

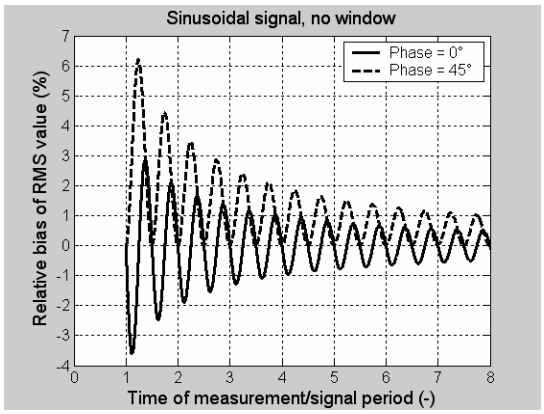

Fig 1a.

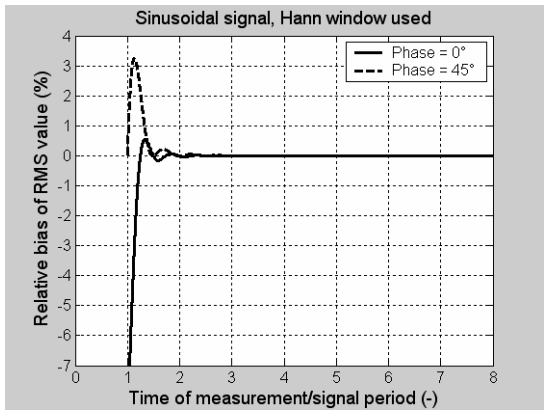

Fig 1b.

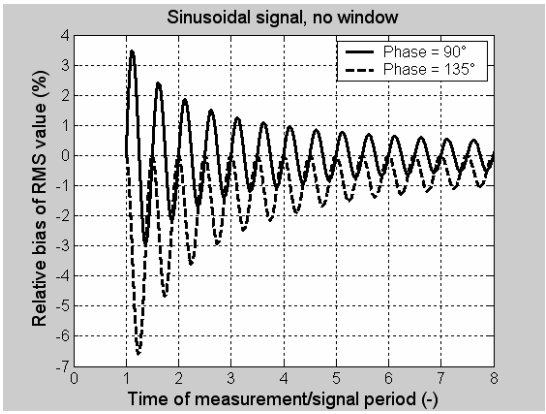

Fig 2a.

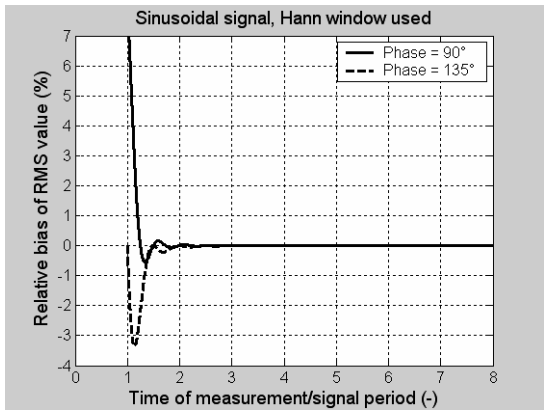

Fig 2b.

Bias of RMS depends on phase related to starting point of sampling (see Fig. 1 and Fig. 2) and type of window. Suppression of bias is higher for higher-order windows used and higher number of signal periods sampled. The large bias for low number of periods sampled is caused by violation of the condition of correct use of window - more than $2P + 1$ signal periods should be sampled (see Fig. 1, Fig. 2 and Tab. 1). The grey background of table cells indicates cases of violation of the condition mentioned and M is number of integer periods sampled in the measured interval $T_M = (M+\lambda)\cdot T_{sig}$.

Table 1. Comparison of RMS value bias for different windows for sinusoidal signal with $\varphi = 0$

Window	P	Maximal bias (%)					
		$M > 1$	$M > 2$	$M > 3$	$M > 5$	$M > 7$	$M > 10$
Rectangular (no window)	0	–3.6	–1.9	–1.3	–0.8	–0.6	–0.4
Hann	1	–8.7	–0.032	–0.004	$-3\cdot10^{-4}$	$-5.5\cdot10^{-5}$	$-1\cdot10^{-5}$
Hamming	1	–6.9	–0.035	–0.018	–0.012	$-9\cdot10^{-3}$	$-6.5\cdot10^{-3}$
Blackman	2	–17	–0.26	$-3.7\cdot10^{-4}$	$-3.6\cdot10^{-5}$	$-7.7\cdot10^{-6}$	$-1.4\cdot10^{-6}$
4Term **Blackman–Harris**	3	–25	–1.5	$-6.3\cdot10^{-3}$	$-6\cdot10^{-7}$	$-1.1\cdot10^{-7}$	$-2.5\cdot10^{-8}$
5Term **Blackman–Harris**	4	–30	–3.3	–0.07	$-3.8\cdot10^{-8}$	$-3.8\cdot10^{-9}$	$-1\cdot10^{-9}$

IV. Multi-frequency signals

The previous formulae of bias of RMS value estimation were derived for sinusoidal signal. Formulae can be generalized for the case of multi-frequency signal.

A. Rectangular window (no window used)

For signal containing higher spectral components the estimated value of RMS can be expressed as

$$X'_{RMS} = \sqrt{\sum_{i=1}^{N} X_{RMS_i}^2 \left(1+\delta\left(X_{RMS_i}\right)\right)^2 + \sum_{i=1}^{N-1}\sum_{j=i+1}^{N} \Delta_{(i,j)}} \tag{8}$$

The bias of individual spectral components in (8) can by found as

$$\delta\left(X_{RMS_i}\right) = \sqrt{1 - \frac{\sin\left(4\pi i\left(M+\lambda\right)+2\varphi_i\right) - \sin\left(2\varphi_i\right)}{4\pi i\left(M+\lambda\right)}} - 1 \tag{9}$$

and term providing mutual influence of these components can be given by

$$\Delta_{(i,j)} = 2X_{RMS_i}X_{RMS_j}\left(\frac{\sin\left((i-j)2\pi\lambda+\left(\varphi_i-\varphi_j\right)\right)-\sin\left(\varphi_i-\varphi_j\right)}{(i-j)2\pi\lambda(M+\lambda)} - \frac{\sin\left((i+j)2\pi\lambda+\left(\varphi_i+\varphi_j\right)\right)-\sin\left(\varphi_i+\varphi_j\right)}{(i+j)2\pi\lambda(M+\lambda)}\right) \tag{10}$$

Verification of this relation by numerical simulation for the case of periodical test signal containing the first four harmonic components with amplitudes V_i and phases φ_i (V_1=1, $\varphi_1 = \pi/4$; V_2=0.5, $\varphi_2 = \pi/2$; V_3=0.3, $\varphi_3 = \pi/4$; V_4=0.1, $\varphi_4 = \pi/2$) is show in Fig. 3.

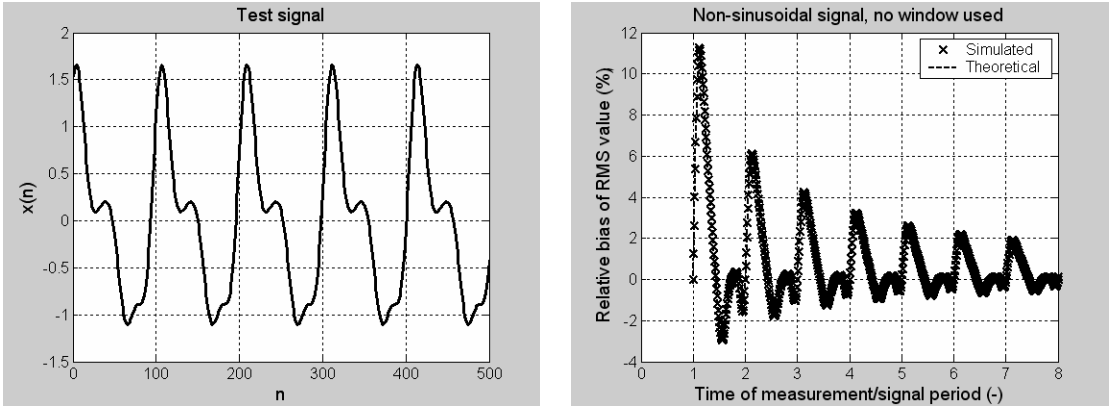

Fig. 3. Non-sinusoidal signal and corresponding RMS value bias

B. Cosine windows

An analogous procedure could be applied for the case of signal windowing using cosine windows. The estimation of RMS value is composed here again of individual components and terms representing the mutual influence of these components and is given in this case by

$$X'_{RMS} = \sqrt{\sum_{i=1}^{N} X_{RMS_i}^2 \left(1+\delta_w\left(X_{RMS_i}\right)\right)^2 + \sum_{i=1}^{N-1}\sum_{j=i+1}^{N} \Delta_{w(i,j)}} \tag{11}$$

The bias δ_w of individual components can be estimated using (6) (it should be taken into account that number of sampled periods of the i-th component is i-times number of sampled periods of signal ($M+\lambda$)). The "mutual components" can be expressed here as

$$\Delta_{w(i,j)} = \frac{4X_{RMS_i}X_{RMS_j}}{NNPG\times(M+\lambda)} \int_0^{(M+\lambda)} w^2(t)\sin(i2\pi t+\varphi_i)\sin(j2\pi t+\varphi_j)dt \tag{12}$$

This relation can be expressed in the form similar to (6) but in that form it is so complicated that it is not presented here.

The comparison of the classical method and the new method using Hann window for the rectangular pulse train (with maximum value 1, minimum value 0 and duty cycle 1:1) and triangular signal (with maximum value 1 and minimum value –1) is shown in Fig. 4

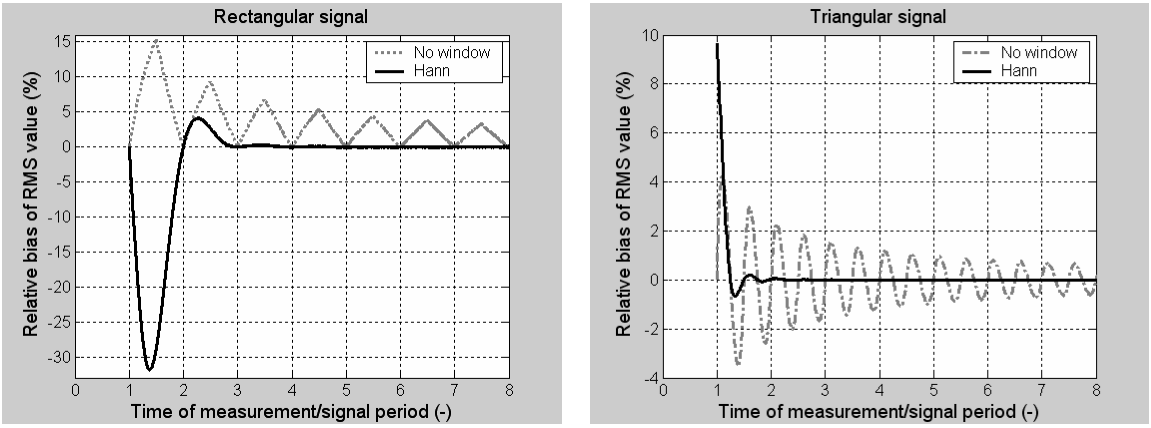

Fig. 4. Comparison of the classical and new methods for rectangular and triangular signal

V. Uncertainty of RMS value due to quantization

Using window influences also uncertainty due to signal quantization. Based on uncertainty propagation law [4] it can be found that this uncertainty component can be expressed as

$$u^2\left(X_{RMS}\right) = u_n^2 \frac{1}{N^2\times nnpg^2}\sum_{n=0}^{N-1} w^4 = \frac{u_n^2\times ENBW_0}{N} \tag{13}$$

where *nnpg* is normalized noise power gain (3)[2], N is number of samples, u_n is standard deviation of quantization or another external noise affecting input samples, and $ENBW_0$ is equivalent-noise bandwidth of the squared window (equal to 1 for rectangular window) and given by [3]

$$ENBW_0 = N\frac{\sum_{n=0}^{N-1} w^4(n)}{\left(\sum_{n=0}^{N-1} w^2(n)\right)^2} \tag{14}$$

The quantization noise of ADC can be expressed as

$$u_n = \frac{V_{range}}{2^{ENOB}\sqrt{12}} \tag{15}$$

where V_{range} is the full-scale range of the used ADC and *ENOB* is its effective number of bits.

The verification of (13) for various window types and numbers of samples is presented in Tab. 2 for the ADC with effective number of bits 8 and full-scale range 10 V. Tab. 2 shows the uncertainty values for both theoretical relation (13) (the first column) and for 5000 numerical simulations (the second column) for each of the 6 given number of samples

Table 2a. Uncertainty component (in volts) caused by quantization for 8-bit ADC with range 10 V

Window	P	Number of samples N					
		64		128		256	
		theoretical	*simulated*	*theoretical*	*simulated*	*theoretical*	*simulated*
Rectangular (no window)	0	$1.41\cdot10^{-3}$	$1.41\cdot10^{-3}$	$9.97\cdot10^{-4}$	$9.97\cdot10^{-4}$	$7.05\cdot10^{-4}$	$7.02\cdot10^{-4}$
Hann	1	$1.97\cdot10^{-3}$	$1.98\cdot10^{-3}$	$1.39\cdot10^{-3}$	$1.4\cdot10^{-3}$	$9.83\cdot10^{-4}$	$9.84\cdot10^{-4}$
Hamming	1	$1.9\cdot10^{-3}$	$1.9\cdot10^{-3}$	$1.34\cdot10^{-3}$	$1.35\cdot10^{-3}$	$9.5\cdot10^{-4}$	$9.48\cdot10^{-4}$
Blackman	2	$2.16\cdot10^{-3}$	$2.17\cdot10^{-3}$	$1.53\cdot10^{-3}$	$1.52\cdot10^{-3}$	$1.08\cdot10^{-3}$	$1.09\cdot10^{-3}$
4Term **Blackman–Harris**	3	$2.34\cdot10^{-3}$	$2.34\cdot10^{-3}$	$1.66\cdot10^{-3}$	$1.67\cdot10^{-3}$	$1.17\cdot10^{-3}$	$1.19\cdot10^{-3}$
5Term **Blackman–Harris**	4	$2.49\cdot10^{-3}$	$2.47\cdot10^{-3}$	$1.75\cdot10^{-3}$	$1.76\cdot10^{-3}$	$1.24\cdot10^{-3}$	$1.24\cdot10^{-3}$

Table 2b. Uncertainty component (in volts) caused by quantization for 8-bit ADC with range 10 V

Window	P	Number of samples N					
		512		1024		2048	
		theoretical	*simulated*	*theoretical*	*simulated*	*theoretical*	*simulated*
Rectangular (no window)	0	$4.98\cdot10^{-4}$	$4.97\cdot10^{-4}$	$3.52\cdot10^{-4}$	$3.51\cdot10^{-4}$	$2.49\cdot10^{-4}$	$2.48\cdot10^{-4}$
Hann	1	$6.95\cdot10^{-4}$	$6.94\cdot10^{-4}$	$4.91\cdot10^{-4}$	$4.93\cdot10^{-4}$	$3.47\cdot10^{-4}$	$3.48\cdot10^{-4}$
Hamming	1	$6.72\cdot10^{-4}$	$6.71\cdot10^{-4}$	$4.75\cdot10^{-4}$	$4.73\cdot10^{-4}$	$3.36\cdot10^{-4}$	$3.38\cdot10^{-4}$
Blackman	2	$7.63\cdot10^{-4}$	$7.61\cdot10^{-4}$	$5.4\cdot10^{-4}$	$5.38\cdot10^{-4}$	$3.82\cdot10^{-4}$	$3.86\cdot10^{-4}$
4Term **Blackman–Harris**	3	$8.28\cdot10^{-4}$	$8.26\cdot10^{-3}$	$5.86\cdot10^{-4}$	$5.86\cdot10^{-4}$	$4.14\cdot10^{-4}$	$4.14\cdot10^{-4}$
5Term **Blackman–Harris**	4	$8.74\cdot10^{-4}$	$8.71\cdot10^{-4}$	$6.18\cdot10^{-4}$	$6.15\cdot10^{-4}$	$4.37\cdot10^{-4}$	$4.34\cdot10^{-4}$

VI. Influence of approximation of integral

Replacing integration by summation results in additional bias of the RMS value estimation. This part of bias is not significant for the case of high enough number of samples per period. Previous formulae were obtained for the case, when influence of integration approximation was not considered. Relation for considering this effect for the case of rectangular window has the following form

$$\delta_{RMS} = \left(\sqrt{1 - \frac{1}{N} \sum_{n=0}^{N-1} \cos\left(\frac{4\pi(M+\lambda)}{N} + 2\varphi \right)} - 1 \right) \cdot 100\% \tag{16}$$

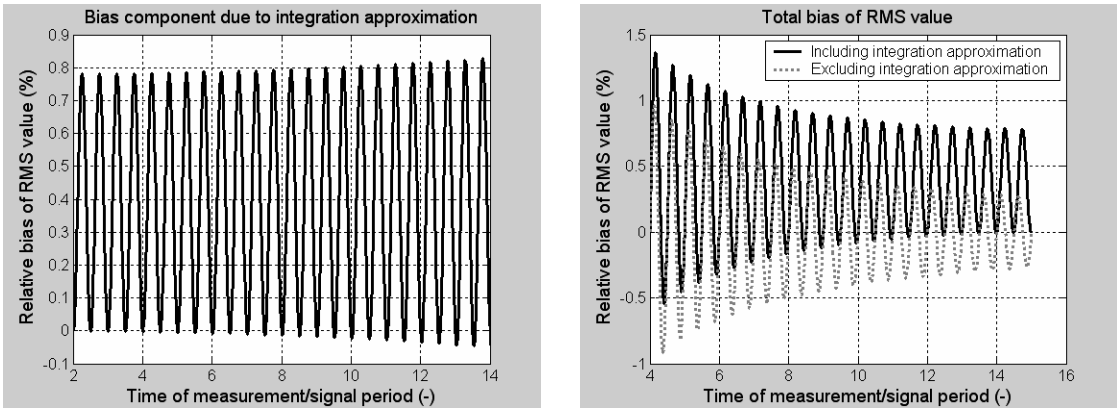

Fig. 5. Influence of integration approximation on RMS estimation

Fig. 5 shows the bias component due to integration approximation and the total bias both with and without the influence of integration approximation. All dependences are plotted for total number of

samples N = 64. Our experiments shown that maximum bias caused by integration for the same conditions using Hann window is in the order of 10^{-7} % and can therefore be disregarded.

VII. Measurement

Several measurements to verify the presented theory were performed. Examples of these measurements are presented in Fig. 6. (sinusoidal signal, V_{max}=*0.5 V,* without DC component, N=128, sampling frequency 1 kHz, ADC ENOB 12 bit (achieved by dithering), ADC range -5V to 5V, trigger level 0 V (it corresponds to $\varphi = 0°$), 100 measurement repetitions for each measured value).

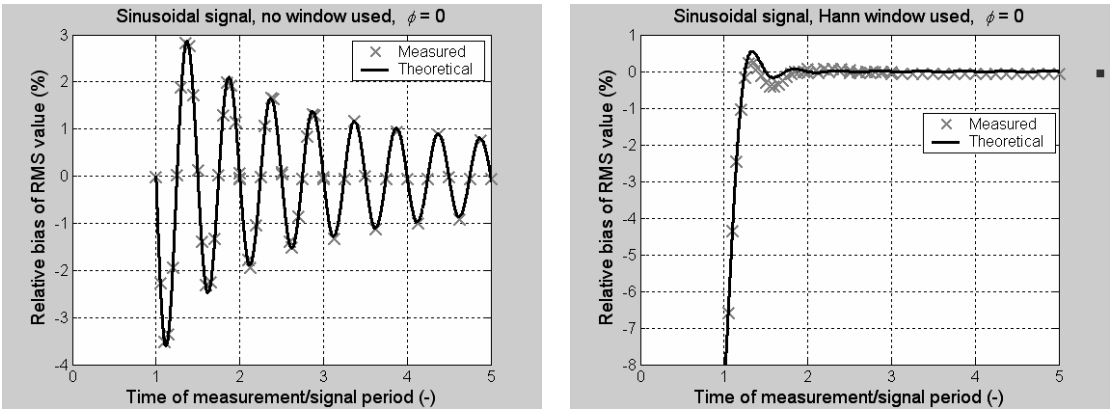

Fig. 6. Measurement validation of theoretical results for rectangular and Hann window

VIII. Conclusions

The efficiency of the described method can be seen from the presented figures and tables. The reduction of RMS estimation bias depends on the type of the used window. The higher the window order, the higher the suppression of RMS estimation bias. However, as can be seen from Tab. 1, even the first order windows application is very efficient compared to the classical method. On the other hand uncertainty component caused by signal quantization increases slightly with window order (see Tab. 2). The method is simple and fast as compared to the classical one and to RMS finding in frequency domain. Compared to finding RMS value in the frequency domain by means of evaluation of energy within the window spectrum main lobe the presented method leads to much higher accuracy of RMS value estimation [1]. This method does not allow however finding only the RMS values of selected components.

Acknowledgement

This research was supported by the research program No. MSM6840770015 "Research of Methods and Systems for Measurement of Physical Quantities and Measured Data Processing " of the CTU in Prague sponsored by the Ministry of Education, Youth and Sports of the Czech Republic and program No. 102/05/H032 "Research, development and optimization of measuring systems and measurement uncertainty estimation by their application" of the CTU in Prague, sponsored by Grant Agency of the Czech Republic.

References

[1] M. Novotny, M. Sedlacek, "Measurement of RMS values of non-coherently sampled signals*",* *Proc. of 13th international IMEKO TC-4 Symposium Athens*, Greece, October 2004, pp.230-235

[2] F. J. Harris, "On the use of windows for harmonic analysis with discrete Fourier transform", *Proc. IEEE*, vol.66, pp.51-83, 1978

[3] P. Carbone, E. Nunzi, D. Petri, "Windows for ADC dynamic testing via frequency-domain analysis", *IEEE Transaction on instrumentation and measurement*, vol. 50, no. 6, December 2001, pp. 1571-1575

[4] *Guide to the Expression of Uncertainty in Measurements*, International Organization for Standardization, Geneve, 1993